

Article

Evaluation of *Bacillus subtilis* Czk1 Metabolites by LC–MS/MS and Their Antifungal Potential against *Pyrrhoderma noxium* Causing Brow Rot Disease

Yanqiong Liang ¹, Weihuai Wu ¹, Rui Li ¹, Ying Lu ¹, Guihua Wang ², Shibe Tan ¹, Helong Chen ¹, Jingen Xi ¹, Xing Huang ¹, Chunping He ^{1,*} and Kexian Yi ^{3,4,5,6,*}

¹ Environment and Plant Protection Institute, Chinese Academy of Tropical Agricultural Sciences, Haikou 571101, China; yanqiongliang@126.com (Y.L.); weihuaiwu2002@163.com (W.W.); ruili202305@163.com (R.L.); ytluy2010@163.com (Y.L.); tanshibei915@163.com (S.T.); chenhelong951@126.com (H.C.); xijingen@163.com (J.X.); hxalong@gmail.com (X.H.)

² College of Forestry, Hainan University, Haikou 570228, China; wgh8308@163.com

³ Sanya Research Institute of Chinese Academy of Tropical Agricultural Sciences, Sanya 572025, China

⁴ Key Laboratory of Integrated Pest Management on Tropical Crops, Ministry of Agriculture and Rural Affairs, Haikou 571101, China

⁵ Hainan Key Laboratory for Detection and Control of Tropical Agricultural Pests, Haikou 571101, China

⁶ Hainan Engineering Research Center for Biological Control of Tropical Crops Diseases and Insect Pests, Haikou 571101, China

* Correspondence: hechunppp@163.com (C.H.); yikexian@126.com (K.Y.); Tel.: +86-898-66969238 (C.H.)

Abstract: Brown rot disease caused by *Pyrrhoderma noxium* is a widespread disease that severely affects the roots of rubber trees (*Hevea brasiliensis* Muell. Arg.). The economic losses, along with environmental and health problems arising from the use of disease control chemicals, have raised the interest of scholars to explore the use of biological control agents for the effective control of fungal pathogen *P. noxium*. Here, the inhibition effect of the culture filtrate of *B. subtilis* Czk1 on *P. noxium* was demonstrated. The findings indicate that the antifungal activity of this strain is mediated wholly or partly by compounds produced in the culture filtrate. The combined use of liquid chromatography–tandem mass spectrometry and antifungal activity assays rapidly identified compounds produced by *B. subtilis* Czk1. Metabolic profiles were assessed and used to identify major metabolites based on the scores of variable importance in the projection and the plot scores of principal component analysis. A total of 296 differential metabolites were screened, including 208 in positive ion mode and 88 in negative ion mode. Two key metabolites, diacetyl and trans-2-octenoic acid, were screened from 29 metabolites by antifungal activity assays. The median effective concentration (EC₅₀) of trans-2-octenoic acid and diacetyl were 0.9075 mg/mL and 4.8213 mg/mL, respectively. The antifungal metabolites can disrupt the internal structure of the pathogenic fungal mycelium, thereby impeding its growth. This study is expected to contribute to the existing knowledge of Czk1-produced metabolites and their future antifungal applications. This study is also expected to provide a new biopreservative perspective on unexplored antifungal metabolites produced by Czk1 as a biocontrol agent.

Keywords: *Bacillus subtilis* Czk1; liquid chromatography–tandem mass spectrometry; antifungal metabolites; *Pyrrhoderma noxium*



Citation: Liang, Y.; Wu, W.; Li, R.; Lu, Y.; Wang, G.; Tan, S.; Chen, H.; Xi, J.; Huang, X.; He, C.; et al. Evaluation of *Bacillus subtilis* Czk1 Metabolites by LC–MS/MS and Their Antifungal Potential against *Pyrrhoderma noxium* Causing Brow Rot Disease. *Agriculture* **2023**, *13*, 1396. <https://doi.org/10.3390/agriculture13071396>

Academic Editors: Ying-Hong Lin and Yi-Hsien Lin

Received: 9 June 2023

Revised: 9 July 2023

Accepted: 11 July 2023

Published: 14 July 2023



Copyright: © 2023 by the authors. Licensee MDPI, Basel, Switzerland. This article is an open access article distributed under the terms and conditions of the Creative Commons Attribution (CC BY) license (<https://creativecommons.org/licenses/by/4.0/>).

1. Introduction

Rubber tree (*Hevea brasiliensis* Muell. Arg.) is a perennial crop that is distributed in tropical countries and is considered one of the global commercial sources of high-quality natural rubber [1–3]. Rubber trees are an important crop for the national economies of many developing countries, and they greatly contribute to the welfare of smallholder farmers worldwide [4]. Latex extracted from the stem of rubber trees (*H. brasiliensis*) is widely used in industrial products, including tyres, gloves, containers, shoes, and adhesives [5,6].

Owing to its advantageous physicochemical properties, the natural rubber cannot be easily replaced by synthetic polymers and the global demand is constantly growing, further suggesting its wide range of industrial applications [7,8].

Brown rot disease (BRD), caused by *Pyrrhoderma noxium* (Corner) L.W. Zhou & Y.C. Dai (*Phellinus noxius* (Corner) GH Cunn), is a widespread important disease infecting the root system of rubber trees [9]. The uptake and transport of water and nutrients in the soil are limited by root and butt rot, which result in the aboveground symptoms [10]. *P. noxium* has a broad host spectrum, with over 200 plant species in 59 families that have been reported, including woody and herbaceous species [11–14]. BRD is widespread in tropical and subtropical countries in Southeast Asia, Africa, Oceania, Central America, Japan, and the Caribbean region [15,16]. It also abounds on the tropical island of Hainan in China [11]. Due to the wide host range of the pathogens and its soil-borne nature, BRD is difficult to control. Currently, various forms of BRD are controlled using chemical fungicides. However, these fungicides are expensive and negatively impact on the health of humans, animals, and ecosystems [17,18]. Therefore, biological control may be a more effective and environmentally friendly method for controlling rubber tree rot diseases [19–22].

Bacillus spp. have antagonistic potential against fungal phytopathogens and can be used to produce a variety of antifungal natural products, indicating their wide range of applications in agriculture, food, healthcare, and other industries [23–25]. *Bacillus subtilis* is an important group of microorganisms in agricultural soils and plant rhizospheres [26]. This type of species produces a variety of active compounds, including enzymes, antibiotics, amino acids, and insecticides, that can be used in industry and agriculture [27–29]. *B. subtilis* strains acquire extensive use in biological control of variety of plant diseases, such as wheat sheath blight [30], rice blast [31], litchi anthracnose [32], and late blight disease of potato [33].

Liquid chromatography–tandem mass spectrometry (LC–MS/MS) is a rapid, sensitive, and accurate method for identifying antifungal compounds with a wide range of applications in the life sciences. The LC–MS/MS method is now the preferred method for analyzing metabolomic pathways in microbiology [34,35].

In our previous research, *B. subtilis* Czk1 was isolated from the aerial roots of *H. brasiliensis*. The strain and its fermentation supernatant showed antifungal activity against a variety of fungi pathogenic, including *Ganoderma pseudoferreum*, *Phellinus noxius*, *Helicobasidium compactum*, *Rigidoporus lignosus*, *Sphaerostilbe repens*, and *Colletotrichum gloeosporioides*. The supernatant of *B. subtilis* Czk1 has the characteristics of high temperature resistance and insensitivity to ultraviolet light and protease K [36,37]. In this study, the metabolites of *B. subtilis* Czk1 were identified by LC–MS/MS. To identify the major antifungal compound, different metabolites produced by *B. subtilis* Czk1 were separately tested for their antifungal activity against *P. noxium*. The key compounds produced by *B. subtilis* Czk1 were rapidly identified by combining the use of LC–MS/MS and antifungal activity assays.

2. Materials and Methods

2.1. Microbial Strains and Culture Conditions

B. subtilis strains Czk1 and *P. noxium* were previously isolated from rubber trees in the laboratory of the Environment and Plant Protection Institute (Chinese Academy of Tropical Agricultural Sciences, Haikou, China). *P. noxium* was used to evaluate the antifungal ability of *B. subtilis* Czk1 and its antifungal product. The sample was cultured on potato dextrose agar (PDA) medium (200 g/L potato, 20 g/L dextrose and 15 g/L agar) at 28 °C for 5 days. Then, *B. subtilis* Czk1 was grown at 37 °C overnight in Luria–Bertani (LB) medium and stored at –20 °C in LB broth supplemented with 30% glycerol.

2.2. Metabolite Extraction

Samples were thawed at 4 °C on ice. Then, 100 µL of the sample was extracted in a 1.5 mL microcentrifuge tube with 400 µL of extraction solvent (V methanol: V acetonitrile = 1:1, internal standard: 2-chloro-L-phenylalanine was 5 µg/mL, Shanghai Macklin Biochemical Co., Ltd,

Shanghai, China), followed by being vortexed for 30 s, sonicated for 5 min (incubated in ice water), incubated for 1 h at -20°C to precipitate proteins, and centrifuged at 12,000 rpm for 15 min at 4°C . Then, 425 μL of the fresh supernatant was collected in a 1.5 mL microcentrifuge tube. Before the addition of 100 μL of extraction solvent (V acetonitrile: V water = 1:1, Shanghai Macklin Biochemical Co., Ltd, Shanghai, China) for reconstitution, the extracts were dried in a vacuum concentrator without heating, vortexed for 30 s, ultrasonicated for 10 min (4°C water bath), and centrifuged at 12,000 rpm for 15 min at 4°C . Additionally, 60 μL of the fresh supernatant was put into a 2 mL LC–MS glass vial, and 10 μL was taken from each sample and pooled as quality control samples. Finally, 60 μL of the supernatant was collected for ultrahigh-performance LC (UHPLC, 1290 Infinity LC, Agilent Technologies, Palo Alto, CA, USA)–quadrupole time of flight MS (QTOFMS, Triple TOF 6600, AB SCIEX, Framingham, MA, USA) analysis. LC–MS/MS analyses, data preprocessing, and annotation were performed according to the methods described in the literature [38,39].

2.3. Screening and Analysis of Different Metabolites of *B. subtilis* Czkl

Proteo Wizard software (<http://proteowizard.sourceforge.net/>, accessed on 12 May 2021) was used to convert the original MS data into the mzXML format. The retention times (RT) were then corrected using XCMS (version 3.2) and the peaks were identified, extracted, integrated, and aligned. The data have been analyzed by principal component analysis (PCA) and orthogonal partial least squares (OPLS)–discriminant analysis (DA) using SIMCA software (version 14.1, Sartorius Stedim Data Analytics AB, Umea, Sweden). Variable importance projection (VIP) scores, *p*-values, and difference multiplier values were combined to identify differential metabolites in Czkl. OSL–SMMS software (version 1.0, Dalian Dashuo Information Technology Co., Ltd., Dalian, China) was used to match the self-constructed data and subsequently identify the compound.

2.4. Antifungal Activity of Metabolites of *B. subtilis* Czkl

The antimicrobial activity of the differential metabolites screened by the above method was determined. The pure metabolites were purchased from the Chemical Book (<https://www.chemicalbook.com/ProductIndex.aspx>, accessed on 12 May 2021). The pure products of these compounds were prepared as a 1000 mg/mL solution, and 1 mL of the solution was added to 99 mL PDA plate culture medium to prepare the drug-containing medium and *P. noxium* was inoculated into the center of plate to detect their antifungal activity. Then, the selected and identified metabolites were prepared in PDA plate culture media at concentrations of 0.25, 0.5, 1, 2.5, 5, and 10 mg/mL. The culture medium without metabolites was used as the control. After five days, the growth of the pathogen was observed. The inhibition rate was calculated to verify the metabolites with antifungal activity. Additionally, the median effective concentration (EC_{50}) of antimicrobial compounds was calculated based on toxicity determination. The experiment was repeated three times with 6 replicates per treatment.

2.5. Scanning Electron Microscopy (SEM) Observation

Scanning electron microscopy (SEM) was used to observe the hyphal morphology of the control group and the metabolite treatment group. The mycelia of each group were collected and fixed in 2% glutaraldehyde for 12 h at 4°C . The fixed samples were rinsed thrice with 0.1 M phosphate buffered saline for 10 min; dehydrated with different percentages of ethanol solutions, including 30%, 50%, 80%, 90%, and 100%; transferred to tert-Butyl alcohol; and dried with carbon dioxide in a critical point dryer [40,41].

3. Results

3.1. Analysis of Metabolites in the Fermentation Broth of *B. Subtilis* Czkl

Initially, 3228 peaks were detected, but only 3227 metabolites were retained for analysis according to the relative standard deviation of the denoising method. The missing values in the original data were then filled with half the minimum value. Data analysis

was performed using the internal standard normalization method. The SIMCA software package for PCA and OPLS–DA was used to process the resulting three-dimensional data (including peak number, sample name, and normalized peak area). In particular, PCA was used to extract distributions from the raw data, and supervised OPLS–DA was used to achieve a higher-level group separation to enhance understanding of the variables involved in the classification.

3.1.1. Principal Component Analysis

To observe the difference of metabolites between CK group and *B. subtilis* Czk1 fermentation broth samples, PCA was used on the results of the three assays, and the score chart of the dispersion degree of the CK and Czk1 groups could be obtained. The PCA scores indicate that the Czk1 group can be completely distinguished from the CK group. Within the group, the variables can be gathered together. All samples were within the 95% confidence interval (Figure 1). The relevant parameters of the PCA model are shown in Table 1.

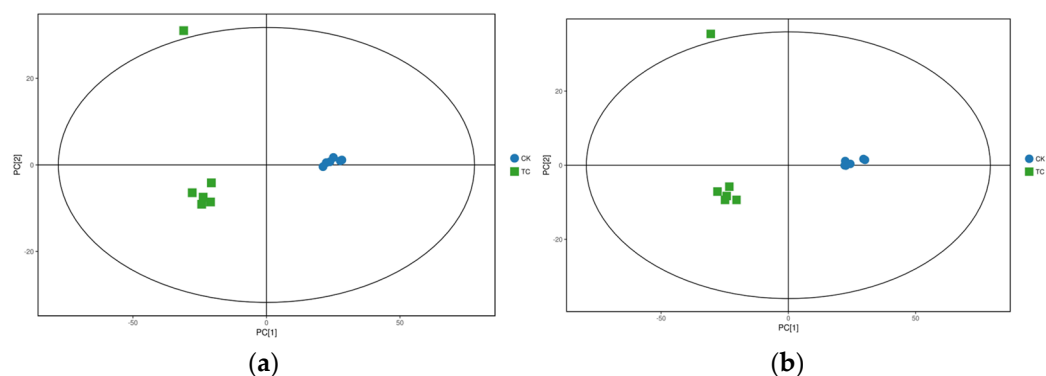


Figure 1. The PCA Score scatter plot in the TC group vs. the CK group ((a): positive ion modes; (b): negative ion modes). Note: the abscissa PC [1] represents the scores of the first principal components, and the ordinate PC [2] represents the scores of second principal components. The blue dots represent the CK group, and the green square represents the TC group.

Table 1. PCA modelling parameters.

Model	Type	A	N	R ² X (cum)	Title
POS	PCA	2	12	0.928	TC vs. CK
NEG	PCA	2	12	0.927	TC vs. CK

Note: Model: model number of SIMCA software modelling; Type: model type of SIMCA; A: Number of principal components of the model; N: number of observations of the model (number of samples); R²X(cum): interpretability of the representative model to the x variable; Title: data object corresponding to the model; POS: positive ion mode; NEG: negative ion mode.

3.1.2. Orthogonal Partial Least Squares-Discriminant Analysis

The cumulative explanatory rates of the OPLS–DA model for each group comparison are shown in Table 2. The OPLS–DA scores for the three assays showed that the Czk1 group was significantly different from the CK group samples in the positive and negative ion modes, and the samples were all within the 95% confidence interval (Figure 2). In this study, the R²Y and Q² were 0.989 and 0.972 in positive ion mode and 0.988 and 0.969 in negative ion mode, respectively. The results further showed that the two models have high explanatory power and predictive power, with an obvious classification effect. Moreover, the metabolites of the two different treatment groups were significantly different. The findings can provide a basis for further analysis and identification.

Table 2. OPLS-DA modelling parameters.

Model	Type	A	N	R ² X (cum)	R ² Y (cum)	Q ² (cum)	Title
POS	OPLS-DA	1 + 1 + 0	12	0.819	0.989	0.972	TC vs. CK
NEG	OPLS-DA	1 + 1 + 0	12	0.811	0.988	0.969	TC vs. CK

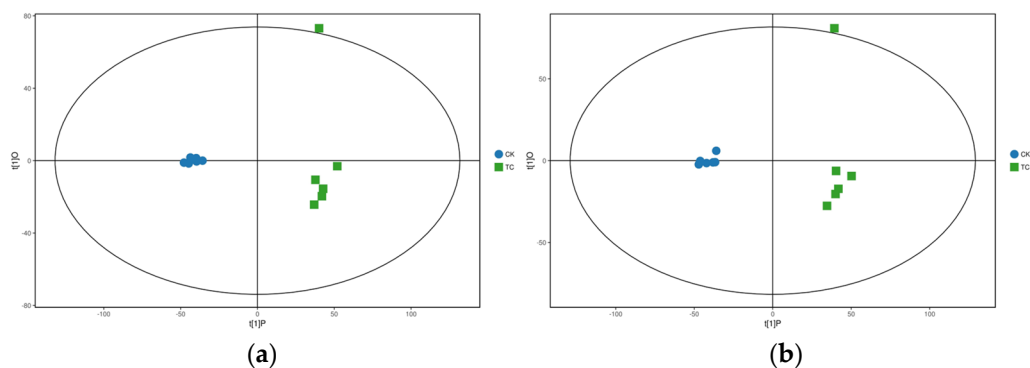


Figure 2. Score scatter plot of the OPLS-DA model for the TC group vs. the CK group ((a): positive ion modes; (b): negative ion modes). Note: the abscissa t [1]P and the ordinate t [1]O represent principal component score of the first principal component and the orthogonal principal component score, respectively. The blue dots represent the CK group, and the green square represents the TC group.

3.1.3. Permutation Test

Here, the permutation test was used to avoid overfitting of the test model and evaluate the statistics of the model, with a particular focus on statistically significant variables. In the replacement test results between Czk1 group versus the CK group in this study (Figure 3), the R²Y of Czk1 group and CK group were 0.1 and 0.3 in the positive and negative ion modes, respectively. The intercept of the Q² regression line and the vertical axis in the positive and negative ion modes is less than zero (−1.11 and −1.26, respectively). As the replacement retention gradually decreases, the proportion of the replaced Y variable increases, whereas the Q² of the random model gradually decreases. Therefore, the original model has good robustness and does not entail overfitting.

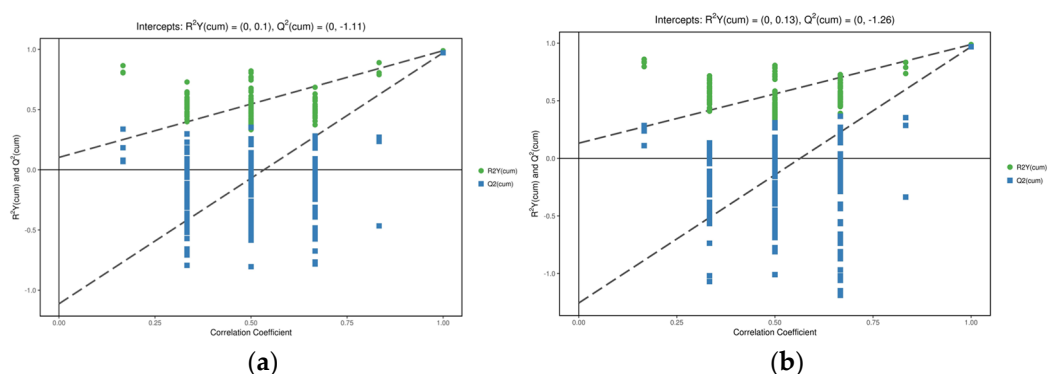


Figure 3. Permutation test of the OPLS-DA model for the TC group vs. the CK group ((a): positive ion modes; (b): negative ion modes). Note: the abscissa represents the replacement retention of the replacement test, and the ordinate represents the value of R²Y or Q². The green dot represents the R²Y value obtained by the permutation test; the blue square dot represents the Q² value obtained by the permutation test; and the two dashed lines represent the regression lines of R²Y and Q², respectively.

3.1.4. Screening and Graphs of Differential Metabolites

The results of the aforementioned two statistical analyses can help users observe both datasets from different angles and draw conclusions. The statistical results can also help users to avoid false positive errors or model overfitting caused by using only one type of

statistical analysis. The card value standards used in this project were $p < 0.05$ in Student's t test and a $VIP > 1$ for the first principal component of OPLS-DA. On this basis, we visualized the screening results of the different metabolites in the form of a volcano plot. The comparative results between the TC and CK groups are shown in Figure 4.

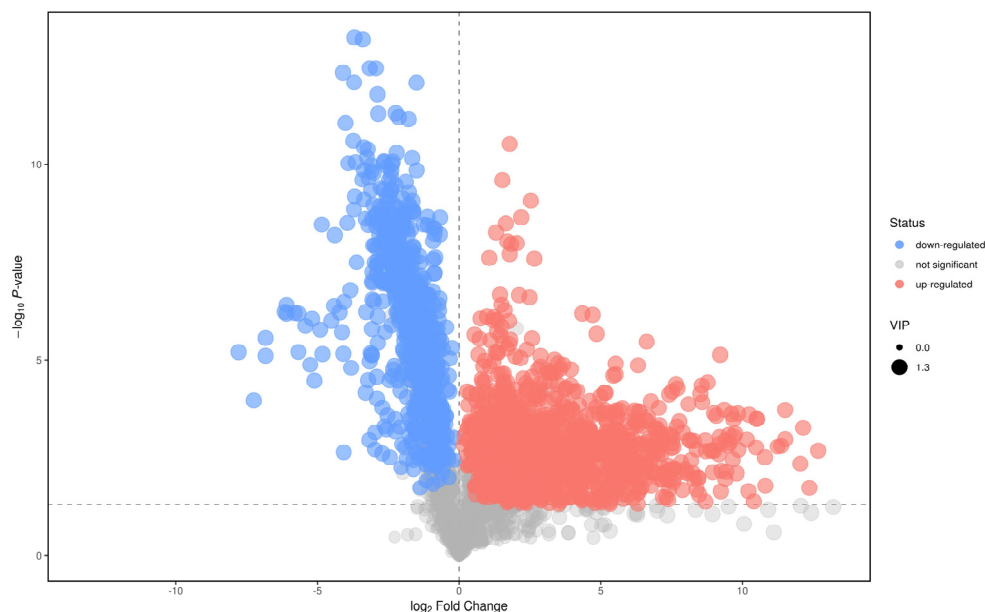


Figure 4. Volcano plot for the TC group vs. the CK group. Note: each dot in the figure represents one metabolite. The multiple changes of each substance in the group (taking the LOG base of 2) is the abscissa, and the p value of the Student's t test (taking the base of 10 for the negative value of the number) is the ordinate. The VIP of the OPLS-DA model is the size of the scatter plot. The larger the scatter point, the higher the VIP value. The red dots are significantly upregulated metabolites; the blue dots are significantly downregulated metabolites; the grey dots are metabolites with no significant difference.

3.2. Identification of Potential Differential Metabolites

The screening threshold criteria used in this study were as follows: $p < 0.05$, $VIP \geq 1$, $FOLD\ CHANGE > 2$ or < 0.05 and matching score > 0.85 . The results revealed different metabolites of CK from the antagonistic Czk1 fermentation broth. A total of 296 differential metabolites were screened, including 208 in positive ion mode and 88 in negative ion mode. The abovementioned compounds were searched in the Chemical Book (<https://www.chemicalbook.com/ProductIndex.aspx>, accessed on 8 April 2021) and screened for metabolites with suspected antimicrobial differences. A total of 29 different metabolites were screened. The differential metabolites produced by *B. subtilis* Czk1 contained amino-acid short peptides, glycosides, purines, amines, bases, esters, alcohols, acids, and other substances. The results are shown in Table 3.

Table 3. Selected metabolites of the Czk1 strain.

Differential Metabolite	MS2-Score	VIP	Q-Value	Fold Change
5-Hydroxyhexanoic acid	0.9045	1.2864	0.00001	15.4119
2-Methylglutaric acid	0.8617	1.2759	0.0006	126.4513
L-2-Aminobutyric acid	0.9700	1.2758	0.0013	31.8914
trans-2-Octenoic acid	0.8521	1.2426	0.0035	4.51206
Phenyllactic acid	0.9254	1.2345	0.0020	3.4718
3-Hydroxycapric acid	0.8604	1.2222	0.00001	0.0335
3-Guanidinopropanoate	0.9199	1.2382	0.0023	6.4467

Table 3. Cont.

Differential Metabolite	MS2-Score	VIP	Q-Value	Fold Change
4-Guanidinobutyric acid	0.9836	1.1470	0.0206	2.9586
Stearic acid	0.9938	1.1215	0.0002	2.5096
Levulinic acid	0.8681	1.0706	0.0101	2.7918
2-Amino-2-methyl-1,3-propanediol	0.8524	1.0991	0.0280	3.7020
Tetramethylpyrazine	0.9621	1.2421	0.00006	2.6826
Tolazoline	0.9169	1.2002	0.0032	3.7448
Methyl acetoacetate	0.9958	1.2743	0.0009	10.9199
Cyclopentolate	0.9701	1.2541	0.0074	67.2024
Glycerol 1-myristate	0.9077	1.2224	0.0183	42.9216
Meclofenoxate	0.8968	1.2287	0.00002	10.5913
Acetoin	0.9066	1.2618	0.0012	9.8972
Diacetyl	0.9002	1.0707	0.0290	2.4256
N-Acetylcadaverine	0.9816	1.1010	0.0175	3.9136
Erucamide	0.9398	1.0369	0.0006	3.9047
Putrescine	0.8668	1.1757	0.0239	9.6776
N,N-Dimethylaniline	0.9495	1.1553	0.0210	3.5936
Dopamine	0.9643	1.2165	0.0053	6.7305
Trimethobenzamide	0.9876	1.2593	0.0004	6.3928
Tamoxifen	0.9979	1.2375	0.0031	14.6384
Amitraz	0.9959	1.2169	0.0013	3.4780
Arecoline	0.9996	1.1740	0.0322	6.9166
Ellipticine	0.9452	1.1621	0.0093	4.2528

3.3. Antifungal Activity of Metabolites

The antagonistic effects of metabolites were evaluated in vitro by using a growth inhibition assay. The inhibitory effect of 29 metabolites on *P. noxium* was significantly different at the concentration of 10 mg/mL. Diacetyl and trans-2-octenoic acid metabolites had the strongest inhibitory effect, and the antifungal rate reached more than 65%, which were 69.85% and 84.32%, respectively, and the inhibition rate of the remaining 27 metabolites was less than 20%. The antifungal effect is shown in the Figure 5. Based on this, the toxicity determination of two antifungal compounds was determined. The results are shown in Figure 6. The median effective concentration (EC₅₀) of trans-2-octenoic acid and diacetyl were 0.9075 mg/mL and 4.8213 mg/mL, respectively. The results are shown in Table 4. As the agent concentration increased, the inhibitory effect of each agent on the BRD pathogen was enhanced. At 1 mg/mL, the inhibition rate of trans-2-octenoic acid was generally less than 50%, but reached 59.65%. When the concentration of diacetyl was 5 mg/mL, the inhibition rate was 50.26%.

Table 4. Toxicity determination of antifungal substances.

Pure Products of Metabolites	Toxicity Regression Equation ($Y = aX + b$)	Correlation Coefficient (r)	Median Effective Concentrations (mg/mL) (EC ₅₀)
trans-2-octenoic acid	$Y = 0.9112x + 5.0384$	0.9820	0.9075
diacetyl	$Y = 0.8506x + 4.4189$	0.9739	4.8213

3.4. Scanning Electron Microscopy Observation

The effect of metabolites on the morphology of *P. noxium* mycelium was studied by SEM. The normal hyphae in the control group had a regular length, smooth surface, and complete structure (Figure 7D). By contrast, the surface of *P. noxium* mycelium treated with metabolites was wrinkled and deformed, and the mycelium ends were swollen. After exposure to the metabolite, the hyphae presented abnormal swelling and branching, and the mycelium ends were swollen (Figure 7A–C). Hence, the metabolites can disrupt the internal structure of the pathogenic fungal mycelium, thereby impeding its growth.

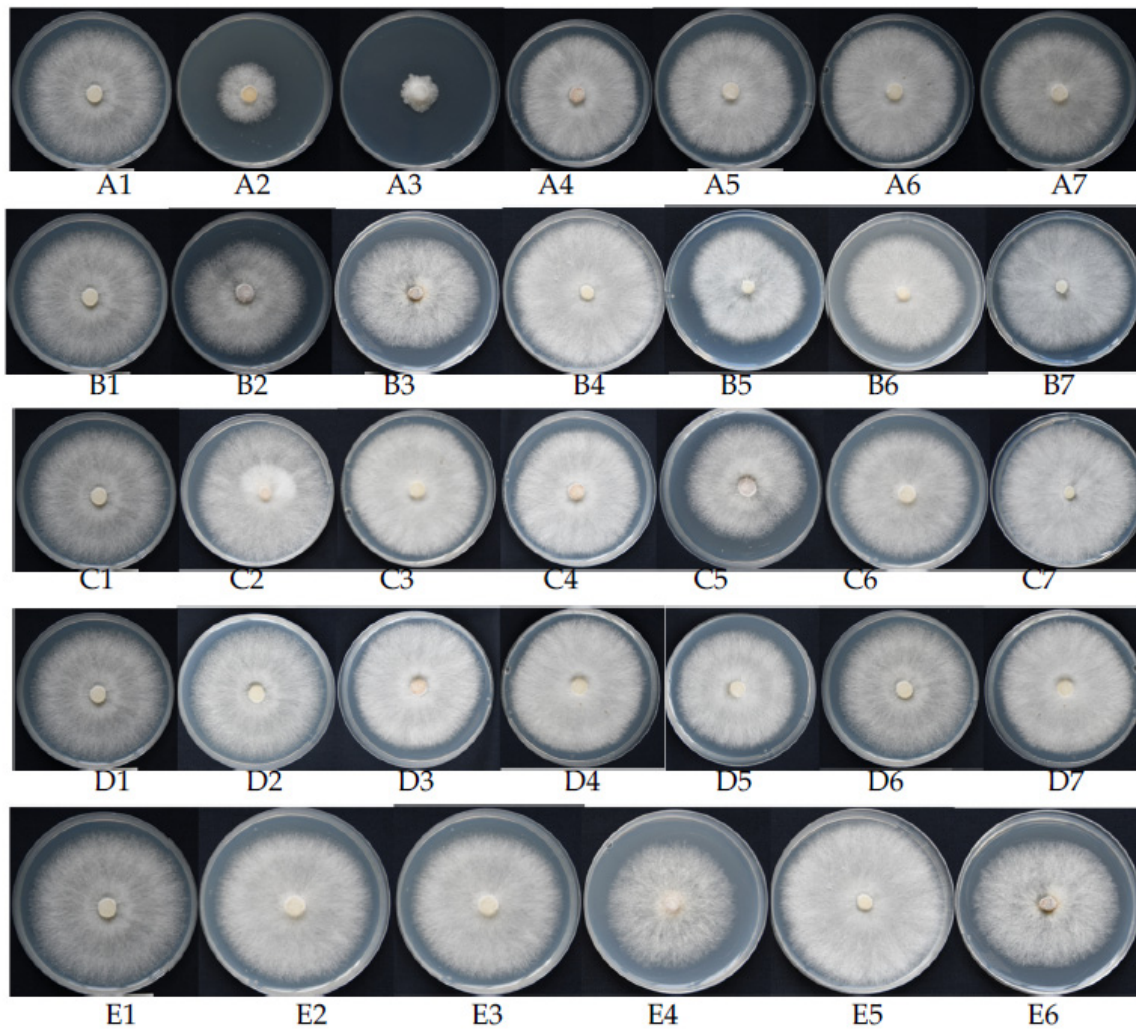


Figure 5. Antifungal activity of 29 metabolites. A1, B1, C1, D1, E1: Control; A2: diacetyl; A3: *trans*-2-octenoic acid; A4: 5-Hydroxyhexanoic acid; A5: 2-Methylglutaric acid; A6: L-2-Aminobutyric acid; A7: Phenyllactic acid; B2: 3-Hydroxycapric acid; B3: 3-Guanidinopropanoate; B4: 4-Guanidinobutyric acid; B5: Stearic acid; B6: Levulinic acid; B7: 2-Amino-2-methyl-1,3-propanediol; C2: Tetramethylpyrazine; C3: Tolazoline; C4: Methyl acetoacetate; C5: Cyclopentolate; C6: Glycerol 1-myristate; C7: Meclofenoxate; D2: Acetoin; D3: *N*-Acetylcadaverine; D4: Erucamide; D5: Putrescine; D6: *N,N*-Dimethylaniline; D7: Dopamine; E2: Trimethobenzamide; E3: Tamoxifen; E4: Amitraz; E5: Arecoline; E6: Ellipticine.

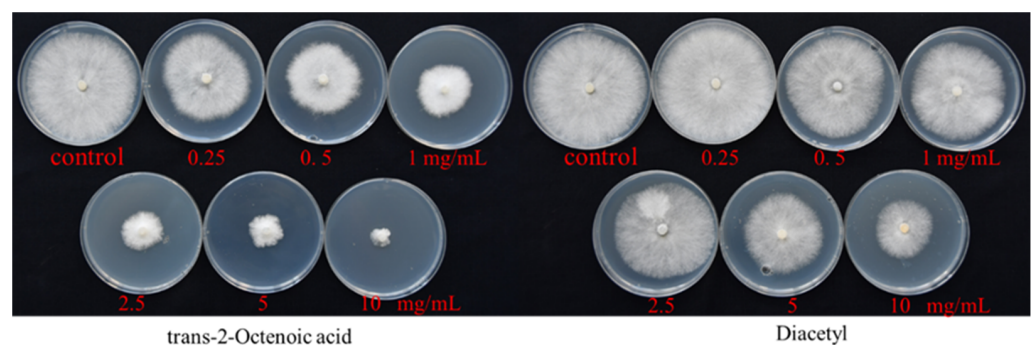


Figure 6. Toxicity determination of two key metabolite pure products.

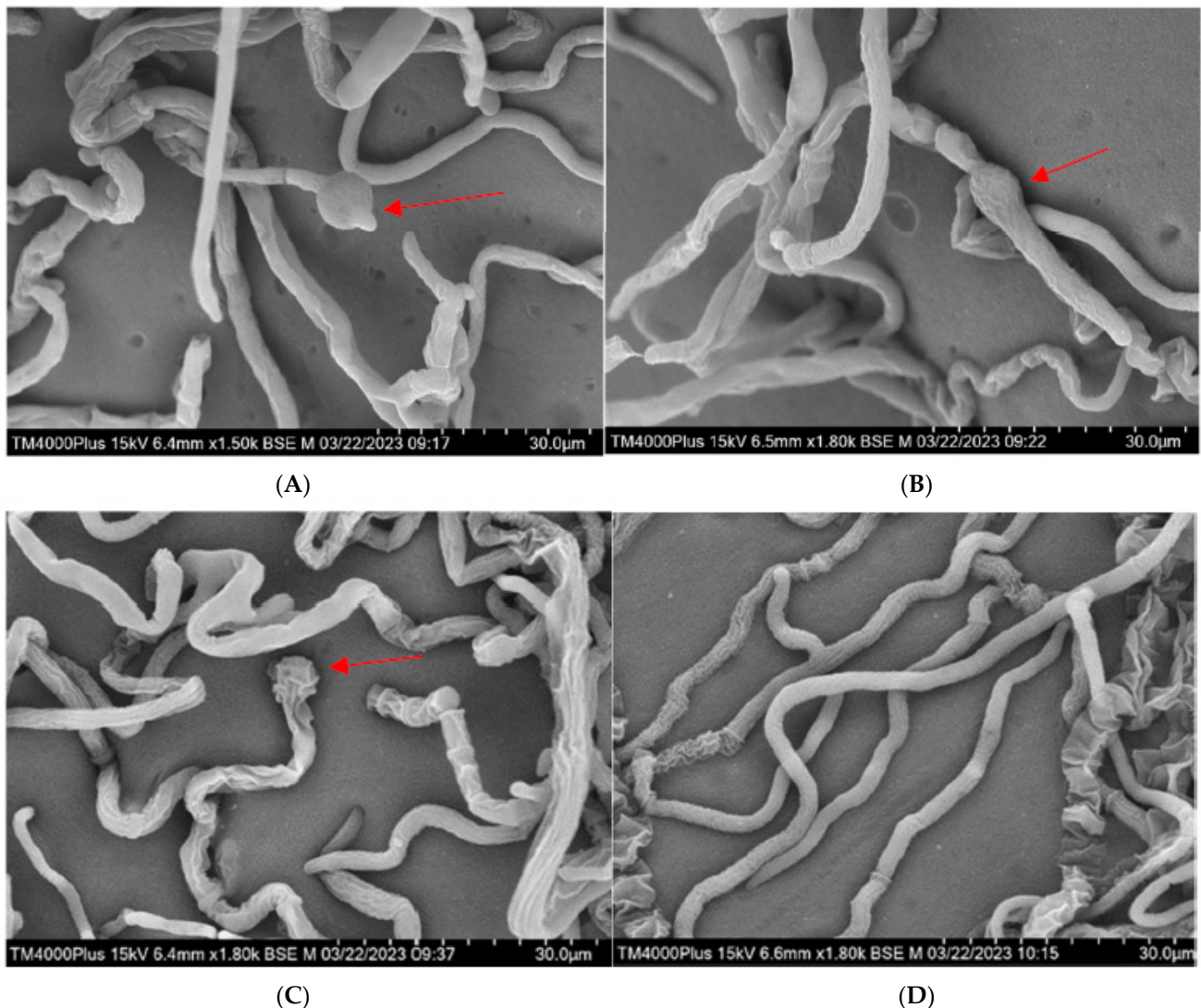


Figure 7. SEM images of *P. noxium* with metabolites ((A–C), metabolites; (D), control).

4. Discussion

Several treatments can be used to manage BRD, including trenching, chemical, and biological control [42–44]. Trenching is a method of creating barriers for BRD spread through interconnected root systems, whereas chemical control is a fast method to control diseases. However, trenching is often difficult to implement or sometimes unsuitable for growing environments. The inappropriate adoption or misuse of chemical fungicides can lead to the appearance of resistant pathogens, which can further threaten human health and the environment [42]. Biological control agents have attracted widespread attention owing to their environmental friendliness, low cost, and versatile mode of action. Chou et al. (2019) analyzed four strains of *Trichoderma* spp. against four strains of *P. noxium* in dual culture and on *Ficus macrocarpa* wood blocks for in vitro antagonism and mycoparasitic abilities [42]. Leung et al. (2020) reported that *Streptomyces padanus* PMS-720 and *Bacillus* sp. BB118 had a good inhibitory effect on *P. noxius* in vitro, and *Bacillus* sp. BB118 could reduce the severity of the disease by up to 50% with only one application [44]. In our previous study, the fermentation supernatant of *B. subtilis* Czkl demonstrated antagonistic activity against *G. pseudoferreum*, *P. noxius*, *H. compactum*, *R. lignosus*, *S. repens*, and *C. gloeosporioides*. We conclude that *B. subtilis* Czkl crude culture supernatant are potential biocontrol agents. Therefore, in this study, we have attempted to investigate the antifungal activity of metabolites produced by *B. subtilis* Czkl culture filtrate that

are involved in the disease. Direct antagonism assays were performed on 29 metabolites screened for antifungal activity; two substances, namely, diacetyl and trans-2-octenoic acid, were screened from the differential metabolites of *B. subtilis* Czk1 to inhibit the pathogen of rubber BRD.

The use of biological agents is currently the best alternative to synthetic fungicides. Several studies have reported the use of microorganisms against plant pathogens. The volatile compounds 2-ethyl-3,6-dimethyl pyrazine, 3-hydroxy-2-butanone (acetoin), benzothiazole, cycloheptasiloxane, and 2-methyl pyrazine produced by *Pseudomonas fluorescens* PDS1 and *B. subtilis* KA9 were found to have inhibitory activity against *Ralstonia solanacearum* by Kashyap et al. (2022) [45]. The protection of lemon fruit against *Penicillium digitatum* by *Schwanniomyces vanriijiae* and 3% ethanolic extracts of propolis in an antagonistic mixture was studied by Abo-Elyousr et al. (2021) [46]. The 80% concentration culture filtrates of *Galactomyces geotrichum* (AUN-AH14) and *G. geotrichum* (AUN-AH23) showed the highest inhibitory effect on the mycelial growth of *Aspergillus niger*, reported by Bagy Hadeel et al. (2023) [47]. In agriculture, *Bacillus* spp. have been extensively used as biological control agents. The production of secondary metabolites with broad antimicrobial activity and highly differentiated structures are some of the interesting properties of *Bacillus* spp. [48–51]. *Bacillus* strains with significant potential to produce antifungal compounds are an important research field. *Bacillus* is capable of secreting several types of antimicrobial compounds, such as polyketides, non-ribosomal produced peptides, terpenoids, and ribosomal synthetic and post-translationally modified peptides, which have varying levels of inhibitory activity against pathogens [52,53]. Several research groups have reported lipopeptides produced by *Bacillus* spp. with antimicrobial activity against a wide range of phytopathogens. Wu et al. (2021) found that two analogs of fengycin B, which exhibited antifungal activity against *Alternaria brassicicola* by inducing swollen hyphae immediately after spore germination, were identified from cell-free culture filtrates of *B. subtilis* PMB102 [54]. Kupper et al. (2019) used LC-MS analysis to show that *B. subtilis* ACB-83 produces two antibiotics, iturin and surfactin, which have inhibitory effects on *Phyllosticta citricarpa* [55]. In the present study, the compounds diacetyl and trans-2-octenoic acid were identified from the culture filtrate of *B. subtilis* Czk1, and were shown to have antifungal activity against *P. noxium*, which belong to ketones and acids, respectively. The results of this experiment are different from those screened by previous researchers, but it does not mean that Czk1 does not have lipopeptide-like antimicrobial compounds. The presence of lipopeptides in *B. subtilis* Czk1 needs to be further investigated due to the abundance of antagonistic metabolites.

Guevara-Avenidaño et al. (2022) showed that BuOH and AcOEt, two diffusible compounds extracted from *Bacillus* spp. INECOL-4742 and INECOL-5927, inhibited the mycelial growth of *Fusarium solani* and *F. kuroshium*. The inhibition rate of BuOH extract B1-Bu on *F. solani* at a concentration of 1 mg/mL was 45% [56]. Pang et al. (2021) reported that antifungal protein chitosanase SH 21 produced by *B. subtilis* SH21 inhibited the growth of *F. solani*. The minimum inhibitory concentration of chitosanase SH21 against *F. solani* was 68 µg/mL [57]. In this work, trans-2-octenoic acid, the antifungal compound, was identified from the culture filtrate of *B. subtilis* Czk1, and the inhibition rate on *P. noxium* reached 59.65% at 1 mg/mL. Bioactive compounds produced by *Bacillus* species have a wide functional variability and broad spectrum of antifungal activity.

Zahari et al. (2022) reported that CRD4, an antifungal compound isolated from *Catharanthus roseus*, had effective biological activities against the growth of *Rigidoporus microporus* and *Ganoderma philippii*, except for *P. noxium* [58]. Panchalingam et al. (2022) found that the volatile and diffusible compounds produced by *Trichoderma* strains #5001 and #5029 had a significant inhibitory effect on the growth of *P. noxium* [59]. There are few studies on the antifungal effect of key metabolites in the culture filtrate on *P. noxium*. The results obtained in this work suggest that the antifungal effect of the strain *B. subtilis* Czk1 on *P. noxium* is related to the action of metabolite microorganisms, and their metabolites can be used as an alternative method to reduce the field impact of chemical fungicide.

To identify the active metabolites of antagonistic bacteria, it is necessary to analyze and identify the substances that actually contribute to their metabolites. LC–MS/MS is a high-sensitivity analytical technique that uses the LC method to separate compounds in samples and analyses the findings using the MS method. In targeted formats, LC–MS/MS can be used to detect and quantify known compounds or metabolites identified from established metabolome databases for a specific sample type [60]. Magan et al. (2019) used LC–MS analysis to identify 46 individual metabolite compounds (47 in total) in skim milk powder and whey protein samples [60]. Deng et al. (2017) detected surfactin and iturin in a mixture of standards by using LC–MS/MS [36]. The detection of secondary metabolites and antimicrobial peptides has been primarily based on their extraction from culture media, as they often have an inhibitory effect on other bacteria and fungi [61]. On this basis, the present study is a rapidly and sensitive method for determining the differential metabolites of *B. subtilis* Czk1 by LC–MS/MS, and a total of 296 differential metabolites were screened. Through the antifungal activity assay, the two compounds with an antifungal effect on *P. noxium* were screened out as diacetyl and trans-2-octenoic acid.

5. Conclusions

The growth of BRD in this work was inhibited after treatment with the culture filtrate of *B. subtilis* Czk1. The antifungal activity of this strain was entirely or partially mediated by compounds produced in the culture filtrate. Furthermore, metabolic profiles were assessed and used as a basis for identifying major metabolites based on VIP scores and PCA plot scores. The main key metabolites identified in the antifungal activity were diacetyl and trans-2-octenoic acid. The antifungal activity assays showed that the *B. subtilis* Czk1 culture filtrate and key metabolites had a significant suppressive activity against *P. noxium*. The results can extend the knowledge on the use of *B. subtilis* Czk1 and its antifungal agents to control plant diseases. We demonstrated that the substances produced by *B. subtilis* have great potential for use as biologically synthesized fungicides in agricultural fields. This research is expected to provide a basis for the future research and the development of biological fungicides. Future efforts will focus on optimizing fermentation conditions to produce a wide range of bioactive compounds and applying antifungal compounds in the field.

Author Contributions: Conceptualization, K.Y. and C.H.; data curation, Y.L. (Yanqiong Liang), W.W., R.L., Y.L. (Ying Lu), S.T., and G.W.; formal analysis, Y.L. (Yanqiong Liang), W.W., S.T., H.C., J.X., X.H. and C.H.; funding acquisition, K.Y.; methodology, Y.L. (Yanqiong Liang), W.W., R.L., Y.L. (Ying Lu), G.W., H.C., X.H. and J.X.; project administration, K.Y. and C.H.; supervision, C.H.; visualization, Y.L. (Yanqiong Liang), K.Y. and C.H.; writing—original draft, Y.L. (Yanqiong Liang), K.Y. and C.H.; writing—review and editing, Y.L. (Yanqiong Liang), K.Y. and C.H. All authors have read and agreed to the published version of the manuscript.

Funding: This research was funded by Hainan provincial Natural Science Foundation of China (320MS083, 322QN360, 320RC692), the specific research fund of The Innovation Platform for Academicians of Hainan Province (SQ2020PTZ0011) and the Earmarked Fund for China Agriculture Research System (CARS-33-BC1).

Institutional Review Board Statement: Not applicable.

Data Availability Statement: Not applicable.

Conflicts of Interest: The authors declare no conflict of interest.

References

1. Venkatachalam, P.; Jayashree, R.; Rekha, K.; Sushmakumari, S.; Sobha, S.; Kumari Jayasree, P.; Kala, R.G.; Thulaseedharan, A. Rubber Tree (*Hevea brasiliensis* Muell. Arg). *Methods Mol. Biol.* **2006**, *344*, 153–164. [[CrossRef](#)] [[PubMed](#)]
2. Lau, N.S.; Makita, Y.; Kawashima, M.; Taylor, T.D.; Kondo, S.; Othman, A.S.; Shu-Chien, A.C.; Matsui, M. The rubber tree genome shows expansion of gene family associated with rubber biosynthesis. *Sci. Rep.* **2016**, *6*, 28594. [[CrossRef](#)] [[PubMed](#)]

3. Jayashree, R.; Nazeem, P.A.; Rekha, K.; Sreelatha, S.; Thulaseedharan, A.; Krishnakumar, R.; Kala, R.G.; Vineetha, M.; Leda, P.; Jinu, U.; et al. Over-expression of 3-hydroxy-3- methylglutaryl-coenzyme A reductase 1 (hmgr1) gene under super-promoter for enhanced latex biosynthesis in rubber tree (*Hevea brasiliensis* Muell. Arg.). *Plant Physiol. Biochem.* **2018**, *127*, 414–424. [[CrossRef](#)] [[PubMed](#)]
4. Cai, Z.; Li, G.; Lin, C.; Shi, T.; Zhai, L.; Chen, Y.; Huang, G. Identifying pathogenicity genes in the rubber tree anthracnose fungus *Colletotrichum gloeosporioides* through random insertional mutagenesis. *Microbiol. Res.* **2013**, *168*, 340–350. [[CrossRef](#)]
5. Oghenekaro, A.O.; Miettinen, O.; Omorusi, V.I.; Evueh, G.A.; Farid, M.A.; Gazis, R.; Asiegbu, F.O. Molecular phylogeny of *Rigidoporus microporus* isolates associated with white rot disease of rubber trees (*Hevea brasiliensis*). *Fungal Biol.* **2014**, *118*, 495–506. [[CrossRef](#)]
6. Röther, W.; Birke, J.; Grond, S.; Beltran, J.M.; Jendrossek, D. Production of functionalized oligo-isoprenoids by enzymatic cleavage of rubber. *Microb. Biotechnol.* **2017**, *10*, 1426–1433. [[CrossRef](#)]
7. Yamashita, S.; Yamaguchi, H.; Waki, T.; Aoki, Y.; Mizuno, M.; Yanbe, F.; Ishii, T.; Funaki, A.; Tozawa, Y.; Miyagi-Inoue, Y.; et al. Identification and reconstitution of the rubber biosynthetic machinery on rubber particles from *Hevea brasiliensis*. *Elife* **2016**, *5*, e19022. [[CrossRef](#)]
8. Manaila, E.; Craciun, G.; Ighigeanu, D.; Lungu, I.B.; Dumitru Grivei, M.D.; Stelescu, M.D. Degradation by Electron Beam Irradiation of Some Composites Based on Natural Rubber Reinforced with Mineral and Organic Fillers. *Int. J. Mol. Sci.* **2022**, *23*, 6925. [[CrossRef](#)]
9. Zhou, L.W.; Ji, X.H.; Vlasák, J.; Dai, Y.C. Taxonomy and phylogeny of *Pyrrhoderma*: A redefinition, the segregation of *Fulvoderma*, gen. nov., and identifying four new species. *Mycologia* **2018**, *110*, 872–889. [[CrossRef](#)]
10. Mazlan, S.; Md, N.; Wahab, A.; Sulaiman, Z.; Dzarifah, Z.F. Major Diseases of Rubber (*Hevea brasiliensis*) in Malaysia. *Pertanika J. Sch. Res. Rev.* **2019**, *5*, 10–21.
11. Ann, P.J.; Chang, T.T.; Ko, W.H. *Phellinus noxius* Brown Root Rot of Fruit and Ornamental Trees in Taiwan. *Plant Dis.* **2002**, *86*, 820–826. [[CrossRef](#)]
12. Fu, C.H.; Hu, B.Y.; Chang, T.T.; Hsueh, K.L.; Hsu, W.T. Evaluation of dazomet as fumigant for the control of brown root rot disease. *Pest Manag. Sci.* **2012**, *68*, 959–962. [[CrossRef](#)]
13. Chung, C.L.; Huang, S.Y.; Huang, Y.C.; Tzean, S.S.; Ann, P.J.; Tsai, J.N.; Yang, C.C.; Lee, H.H.; Huang, T.W.; Huang, H.Y.; et al. The Genetic Structure of *Phellinus noxius* and Dissemination Pattern of Brown Root Rot Disease in Taiwan. *PLoS ONE* **2015**, *10*, e0139445. [[CrossRef](#)] [[PubMed](#)]
14. Liu, T.Y.; Chen, C.H.; Yang, Y.L.; Tsai, I.J.; Ho, Y.N.; Chung, C.L. The brown root rot fungus *Phellinus noxius* affects microbial communities in different root-associated niches of Ficus trees. *Environ. Microbiol.* **2022**, *24*, 276–297. [[CrossRef](#)] [[PubMed](#)]
15. Sahashi, N.; Akiba, M.; Takemoto, S.; Yokoi, T.; Ota, Y.; Kanzaki, N. *Phellinus noxius* causes brown root rot on four important conifer species in Japan. *Eur. J. Plant Pathol.* **2014**, *140*, 869–873. [[CrossRef](#)]
16. Chung, C.L.; Lee, T.J.; Akiba, M.; Lee, H.H.; Kuo, T.H.; Liu, D.; Ke, H.M.; Yokoi, T.; Roa, M.B.; Lu, M.J.; et al. Comparative and population genomic landscape of *Phellinus noxius*: A hypervariable fungus causing root rot in trees. *Mol. Ecol.* **2017**, *26*, 6301–6316. [[CrossRef](#)] [[PubMed](#)]
17. Jin, J.; Wang, W.; He, R.; Gong, H. Valuing health risk in agriculture: A choice experiment approach to pesticide use in China. *Environ. Sci. Pollut. Res. Int.* **2017**, *24*, 17526–17533. [[CrossRef](#)]
18. Ndayambaje, B.; Amuguni, H.; Coffin-Schmitt, J.; Sibon, N.; Ntawubizi, M.; VanWormer, E. Pesticide Application Practices and Knowledge among Small-Scale Local Rice Growers and Communities in Rwanda: A Cross-Sectional Study. *Int. J. Environ. Res. Public Health* **2019**, *16*, 4770. [[CrossRef](#)] [[PubMed](#)]
19. Bulgari, D.; Montagna, M.; Gobbi, E.; Faoro, F. Green Technology: Bacteria-Based Approach Could Lead to Unsuspected Microbe-Plant-Animal Interactions. *Microorganisms* **2019**, *7*, 44. [[CrossRef](#)]
20. Ogbemor, N.O.; Adekunle, A.T.; Eghafona, O.N.; Ogboghodo, A.I. Biological control of *Rigidoporus lignosus* in *Hevea brasiliensis* in Nigeria. *Fungal Biol.* **2015**, *119*, 1–6. [[CrossRef](#)]
21. Bonaterra, A.; Badosa, E.; Daranas, N.; Francés, J.; Roselló, G.; Montesinos, E. Bacteria as Biological Control Agents of Plant Diseases. *Microorganisms* **2022**, *10*, 1759. [[CrossRef](#)] [[PubMed](#)]
22. Hirozawa, M.T.; Ono, M.A.; Suguiura, I.M.S.; Bordini, J.G.; Ono, E.Y.S. Lactic acid bacteria and *Bacillus* spp. as fungal biological control agents. *J. Appl. Microbiol.* **2023**, *134*, lxac083. [[CrossRef](#)] [[PubMed](#)]
23. Khan, A.R.; Mustafa, A.; Hyder, S.; Valipour, M.; Rizvi, Z.F.; Gondal, A.S.; Yousuf, Z.; Iqbal, R.; Daraz, U. *Bacillus* spp. as Bioagents: Uses and Application for Sustainable Agriculture. *Biology* **2022**, *11*, 1763. [[CrossRef](#)]
24. Liu, C.; Sheng, J.; Chen, L.; Zheng, Y.; Lee, D.Y.; Yang, Y.; Xu, M.; Shen, L. Biocontrol Activity of *Bacillus subtilis* Isolated from *Agaricus bisporus* Mushroom Compost Against Pathogenic Fungi. *J. Agric. Food Chem.* **2015**, *63*, 6009–6018. [[CrossRef](#)] [[PubMed](#)]
25. Zhang, D.; Yu, S.; Yang, Y.; Zhang, J.; Zhao, D.; Pan, Y.; Fan, S.; Yang, Z.; Zhu, J. Antifungal Effects of Volatiles Produced by *Bacillus subtilis* Against *Alternaria solani* in Potato. *Front. Microbiol.* **2020**, *11*, 1196. [[CrossRef](#)] [[PubMed](#)]
26. Jiang, C.; Li, Z.; Shi, Y.; Guo, D.; Pang, B.; Chen, X.; Shao, D.; Liu, Y.; Shi, J. *Bacillus subtilis* inhibits *Aspergillus carbonarius* by producing iturin A, which disturbs the transport, energy metabolism, and osmotic pressure of fungal cells as revealed by transcriptomics analysis. *Int. J. Food Microbiol.* **2020**, *330*, 108783. [[CrossRef](#)]

27. Zhang, L.; Sun, C. Fengycins, Cyclic Lipopeptides from Marine *Bacillus subtilis* Strains, Kill the Plant-Pathogenic Fungus *Magnaporthe grisea* by Inducing Reactive Oxygen Species Production and Chromatin Condensation. *Appl. Environ. Microbiol.* **2018**, *84*, e00445–18. [[CrossRef](#)]
28. Kaspar, F.; Neubauer, P.; Gimpel, M. Bioactive Secondary Metabolites from *Bacillus subtilis*: A Comprehensive Review. *J. Nat. Prod.* **2019**, *82*, 2038–2053. [[CrossRef](#)]
29. Iqbal, S.; Begum, F.; Rabaan, A.A.; Aljeldah, M.; Al Shammari, B.R.; Alawfi, A.; Alshengeti, A.; Sulaiman, T.; Khan, A. Classification and Multifaceted Potential of Secondary Metabolites Produced by *Bacillus subtilis* Group: A Comprehensive Review. *Molecules* **2023**, *28*, 927. [[CrossRef](#)]
30. Zhang, X.; Guo, X.; Wu, C.; Li, C.; Zhang, D.; Zhu, B. Isolation, heterologous expression, and purification of a novel antifungal protein from *Bacillus subtilis* strain Z-14. *Microb. Cell Fact.* **2020**, *19*, 214. [[CrossRef](#)]
31. Li, L.; Li, Y.; Lu, K.; Chen, R.; Jiang, J. *Bacillus subtilis* KLBMPGC81 suppresses appressorium-mediated plant infection by altering the cell wall integrity signaling pathway and multiple cell biological processes in *Magnaporthe oryzae*. *Front. Cell. Infect. Microbiol.* **2022**, *12*, 983757. [[CrossRef](#)] [[PubMed](#)]
32. Wang, K.; Qin, Z.; Wu, S.; Zhao, P.; Zhen, C.; Gao, H. Antifungal Mechanism of Volatile Organic Compounds Produced by *Bacillus subtilis* CF-3 on *Colletotrichum gloeosporioides* Assessed Using Omics Technology. *J. Agric. Food Chem.* **2021**, *69*, 5267–5278. [[CrossRef](#)] [[PubMed](#)]
33. Alfiky, A.; L'Haridon, F.; Abou-Mansour, E.; Weisskopf, L. Disease Inhibiting Effect of Strain *Bacillus subtilis* EG21 and Its Metabolites Against Potato Pathogens *Phytophthora infestans* and *Rhizoctonia solani*. *Phytopathology* **2022**, *112*, 2099–2109. [[CrossRef](#)] [[PubMed](#)]
34. Deng, Q.; Wang, W.; Sun, L.; Wang, Y.; Liao, J.; Xu, D.; Liu, Y.; Ye, R.; Gooneratne, R. A sensitive method for simultaneous quantitative determination of surfactin and iturin by LC-MS/MS. *Anal. Bioanal. Chem.* **2017**, *409*, 179–191. [[CrossRef](#)]
35. Farzand, A.; Moosa, A.; Zubair, M.; Khan, A.R.; Hanif, A.; Tahir, H.; Tahira, H.A.S.; Gao, X.W. Marker assisted detection and LC-MS analysis of antimicrobial compounds in different *Bacillus* strains and their antifungal effect on sclerotinia sclerotiorum. *Biol. Control* **2019**, *133*, 91–102. [[CrossRef](#)]
36. Zhao, L.L.; He, C.P.; Zheng, X.L.; Fan, L.Y.; Zheng, F.C. Effect of *Bacillus subtilis* strain czk1 on different rubber root pathogens and in vitro control of *Colletotrichum gloeosporioides* on rubber leaf. *J. South. Agric.* **2011**, *42*, 740–743.
37. He, C.P.; Fan, L.Y.; Wu, W.H.; Liang, Y.Q.; Li, R.; Tang, W.; Zheng, X.L.; Xiao, Y.N.; Liu, Z.X.; Zheng, F.C. Identification of lipopeptides produced by *Bacillus subtilis* Czk1 isolated from the aerial roots of rubber trees. *Genet. Mol. Res.* **2017**, *16*, gmr16018710. [[CrossRef](#)]
38. Li, R.; Huang, Y.; Wu, J.; Deng, H.; Wang, L.; Zhang, W.; Ding, J. Whole genome analysis and specific PCR primer development for *vibrio corallilyticus*, combined with transcription and metabolome analysis of red spotting disease in the sea urchin, *strongylocentrotus intermedius*. *Aquac. Rep.* **2022**, *22*, 100957. [[CrossRef](#)]
39. Yu, J.Z.; Ying, Y.; Liu, Y.; Sun, C.B.; Dai, C.; Zhao, S.; Tian, S.Z.; Peng, J.; Han, N.P.; Yuan, J.L.; et al. Antifibrotic action of Yifei Sanjie formula enhanced autophagy via PI3K-AKT-mTOR signaling pathway in mouse model of pulmonary fibrosis. *Biomed Pharmacother.* **2019**, *118*, 109293. [[CrossRef](#)]
40. Zhang, D.; Qiang, R.; Zhou, Z.; Pan, Y.; Yu, S.; Yuan, W.; Cheng, J.; Wang, J.; Zhao, D.; Zhu, J.; et al. Biocontrol and Action Mechanism of *Bacillus subtilis* Lipopeptides' Fengycins Against *Alternaria solani* in Potato as Assessed by a Transcriptome Analysis. *Front. Microbiol.* **2022**, *13*, 861113. [[CrossRef](#)]
41. Gao, Q.; Liu, Y.; Xie, J.; Zhao, S.; Qin, W.; Song, Q.; Wang, S.; Rong, C. Bacterial Infection Induces Ultrastructural and Transcriptional Changes in the King Oyster Mushroom (*Pleurotus eryngii*). *Microbiol. Spectr.* **2022**, *10*, e0144522. [[CrossRef](#)] [[PubMed](#)]
42. Chou, H.; Xiao, Y.T.; Tsai, J.N.; Li, T.T.; Wu, H.Y.; Liu, L.D.; Tzeng, D.S.; Chung, C.L. In Vitro and in Planta Evaluation of *Trichoderma asperellum* TA as a Biocontrol Agent Against *Phellinus noxius*, the Cause of Brown Root Rot Disease of Trees. *Plant Dis.* **2019**, *103*, 2733–2741. [[CrossRef](#)] [[PubMed](#)]
43. Burcham, D.C.; Jia, Y.W.; Abarrientos, N.V.; Ali, M.; Schwarze, F. In vitro evaluation of antagonism by *Trichoderma* spp. towards *Phellinus noxius* associated with rain tree (*Samanea saman*) and Senegal mahogany (*Khaya senegalensis*) in Singapore. *bioRxiv* **2017**. [[CrossRef](#)]
44. Leung, K.T.; Chen, C.Y.; You, B.J.; Lee, M.H.; Huang, J.W. Brown Root Rot Disease of *Phyllanthus myrtifolius*: The Causal Agent and Two Potential Biological Control Agents. *Plant Dis.* **2020**, *104*, 3043–3053. [[CrossRef](#)]
45. Kashyap, A.S.; Manzar, N.; Nebapure, S.M.; Rajawat, M.V.S.; Deo, M.M.; Singh, J.P.; Kesharwani, A.K.; Singh, R.P.; Dubey, S.C.; Singh, D. Unraveling Microbial Volatile Elicitors Using a Transparent Methodology for Induction of Systemic Resistance and Regulation of Antioxidant Genes at Expression Levels in Chili against Bacterial Wilt Disease. *Antioxidants* **2022**, *11*, 404. [[CrossRef](#)]
46. Abo-Elyousr, K.A.M.; Al-Qurashi, A.D.; Almasoudi, N.M. Evaluation of the synergy between *Schwanniomyces vanrijae* and propolis in the control of *Penicillium digitatum* on lemons. *Egypt. J. Biol. Pest Control* **2021**, *31*, 66. [[CrossRef](#)]
47. Bagy Hadeel, M.M.K.; Abo-Elyousr, K.A.M.; Hesham, A.E.L.; Sallam Nashwa, M.A. Development of antagonistic yeasts for controlling black mold disease of Onion. *Egypt. J. Biol. Pest Control* **2023**, *33*, 17. [[CrossRef](#)]
48. Liu, J.; Hagberg, I.; Novitsky, L.; Hadj-Moussa, H.; Avis, T.J. Interaction of antimicrobial cyclic lipopeptides from *Bacillus subtilis* influences their effect on spore germination and membrane permeability in fungal plant pathogens. *Fungal Biol.* **2014**, *118*, 855–861. [[CrossRef](#)]

49. Gu, Q.; Yang, Y.; Yuan, Q.; Shi, G.; Wu, L.; Lou, Z.; Huo, R.; Wu, H.; Borriss, R.; Gao, X. Bacillomycin D Produced by *Bacillus amyloliquefaciens* Is Involved in the Antagonistic Interaction with the Plant-Pathogenic Fungus *Fusarium graminearum*. *Appl. Environ. Microbiol.* **2017**, *83*, e01075-17. [[CrossRef](#)]
50. Fira, D.; Dimkić, I.; Berić, T.; Lozo, J.; Stanković, S. Biological control of plant pathogens by *Bacillus* species. *J. Biotechnol.* **2018**, *285*, 44–55. [[CrossRef](#)]
51. Fatima, R.; Mahmood, T.; Moosa, A.; Aslam, M.N.; Shakeel, M.T.; Maqsood, A.; Shafiq, M.U.; Ahmad, T.; Moustafa, M.; Al-Shehri, M. *Bacillus thuringiensis* CHGP12 uses a multifaceted approach for the suppression of *Fusarium oxysporum* f. sp. ciceris and to enhance the biomass of chickpea plants. *Pest Manag. Sci.* **2023**, *79*, 336–348. [[CrossRef](#)] [[PubMed](#)]
52. Tenea, G.N.; Ascanta, P. Bioprospecting of Ribosomally Synthesized and Post-translationally Modified Peptides Through Genome Characterization of a Novel Probiotic *Lactiplantibacillus plantarum* UTNGt21A Strain: A Promising Natural Antimicrobials Factory. *Front. Microbiol.* **2022**, *13*, 868025. [[CrossRef](#)] [[PubMed](#)]
53. Zhou, L.; Song, C.; Muñoz, C.Y.; Kuipers, O.P. *Bacillus cabrialesii* BH5 Protects Tomato Plants Against *Botrytis cinerea* by Production of Specific Antifungal Compounds. *Front. Microbiol.* **2021**, *12*, 707609. [[CrossRef](#)] [[PubMed](#)]
54. Wu, J.J.; Chou, H.P.; Huang, J.W.; Deng, W.L. Genomic and biochemical characterization of antifungal compounds produced by *Bacillus subtilis* PMB102 against *Alternaria brassicicola*. *Microbiol. Res.* **2021**, *251*, 126815. [[CrossRef](#)]
55. Kupper, K.C.; Moretto, R.K.; Fujimoto, A. Production of antifungal compounds by *Bacillus* spp. isolates and its capacity for controlling citrus black spot under field conditions. *World J. Microbiol. Biotechnol.* **2019**, *36*, 7. [[CrossRef](#)]
56. Guevara-Avendaño, E.; Lizette Pérez-Molina, M.; Luis Monribot-Villanueva, J.; Marian Cortazar-Murillo, E.; Ramírez-Vázquez, M.; Reverchon, F.; Antonio Guerrero-Analco, J. Identification of Antifungal Compounds from *Avocado Rhizobacteria* (*Bacillus* spp.) against *Fusarium* spp., by a Bioassay-Guided Fractionation Approach. *Chem. Biodivers.* **2022**, *19*, e202200687. [[CrossRef](#)]
57. Pang, Y.; Yang, J.; Chen, X.; Jia, Y.; Li, T.; Jin, J.; Liu, H.; Jiang, L.; Hao, Y.; Zhang, H.; et al. An Antifungal Chitosanase from *Bacillus subtilis* SH21. *Molecules* **2021**, *26*, 1863. [[CrossRef](#)]
58. Zahari, R.; Halimoon, N.; Ahmad, M.F.; Ling, S.K. Antifungal Compound Isolated from *Catharanthus roseus* L. (Pink) for Biological Control of Root Rot Rubber Diseases. *Int. J. Anal. Chem.* **2018**, *2018*, 8150610. [[CrossRef](#)]
59. Panchalingam, H.; Powell, D.; Adra, C.; Foster, K.; Tomlin, R.; Quigley, B.L.; Nyari, S.; Hayes, R.A.; Shapcott, A.; Kurtböke, D.İ. Assessing the Various Antagonistic Mechanisms of *Trichoderma* Strains against the Brown Root Rot Pathogen *Pyrrhoderma noxium* Infecting Heritage Fig Trees. *J. Fungi* **2022**, *8*, 1105. [[CrossRef](#)]
60. Magan, J.B.; O'Callaghan, T.F.; Zheng, J.; Zhang, L.; Mandal, R.; Hennessy, D.; Fenelon, M.A.; Wishart, D.S.; Kelly, A.L.; McCarthy, N.A. Impact of Bovine Diet on Metabolomic Profile of Skim Milk and Whey Protein Ingredients. *Metabolites* **2019**, *9*, 305. [[CrossRef](#)]
61. Henriksen, N.N.; Lindqvist, L.L.; Wibowo, M.; Sonnenschein, E.C.; Bentzon-Tilia, M.; Gram, L. Role is in the eye of the beholder—the multiple functions of the antibacterial compound tropodithetic acid produced by marine *Rhodobacteraceae*. *FEMS Microbiol. Rev.* **2022**, *46*, fuac007. [[CrossRef](#)] [[PubMed](#)]

Disclaimer/Publisher's Note: The statements, opinions and data contained in all publications are solely those of the individual author(s) and contributor(s) and not of MDPI and/or the editor(s). MDPI and/or the editor(s) disclaim responsibility for any injury to people or property resulting from any ideas, methods, instructions or products referred to in the content.